ISSN 0036-0244, Russian Journal of Physical Chemistry A, 2020, Vol. 94, No. 8, pp. 1596–1602. © Pleiades Publishing, Ltd., 2020.
Russian Text © The Author(s), 2020, published in Zhurnal Fizicheskoi Khimii, 2020, Vol. 94, No. 8, pp. 1195–1201.

STRUCTURE OF MATTER AND QUANTUM CHEMISTRY

Physicochemical Properties of Condensed Products of Interaction between Iron(II) Cations and Permanganate Ions

Yu. G. Khabarov[a,*], **V. A. Veshnyakov**[a], **E. A. Skripnikov**[a], **D. G. Chukhchin**[a], **A. V. Malkov**[b], **and G. V. Pankina**[c]

[a] *Northern (Arctic) Federal University, Arkhangelsk, 163002 Russia*

[b] *Laverov Federal Center for Integrated Arctic Research, Russian Academy of Sciences, Arkhangelsk, 163002 Russia*

[c] *Department of Chemistry, Moscow State University, Moscow, 119991 Russia*

**e-mail: khabarov.yu@mail.ru*

Received September 11, 2019; revised September 11, 2019; accepted September 17, 2019

Abstract—Condensed products are obtained via the partial oxidation of iron(II) cations using potassium permanganate, and their physicochemical properties are studied. Samples obtained at a potassium permanganate-to-iron(II) molar ratio close to stoichiometric in a preparation of magnetite have the greatest relative magnetic susceptibility. It is shown that the initial rate of formation of relative magnetic susceptibility in the range of 30–70°C depends linearly on the inverse thermodynamic temperature. Sedimentation of the synthesized products upon exposure to an external magnetic field is complete within 1–1.5 min. Diffractometry shows that crystalline magnetite samples form at a $KMnO_4$: Fe(II) molar ratio of 0.08–0.18. Magnetic granulometry reveals they have superparamagnetic properties. Under conditions of static sorption, the degree of extraction of chromate ions is 98.7%.

Keywords: iron, permanganate, redox reactions, magnetite, superparamagnets, sorption

DOI: 10.1134/S0036024420080142

INTRODUCTION

Magnetite Fe_3O_4 and ferrites of a number of metals of the composition MFe_2O_4 are magnetically active compounds. The continuing interest in studying them is due to their widespread practical use. In the crystal structure of magnetite, iron(II) cations and some iron(III) cations are arranged in alternating crystallographic layers. Since the magnetic moments of iron(III) cations are compensated for, the overall magnetization is determined by the parallel ordering of the spins of iron(II) cations. Condensation is the main way of synthesizing magnetite-type magnetically active compounds. A procedure based on the condensation of a solution of iron(II) and iron(III) salts in a 1 : 2 ratio with an alkaline reagent is often used to synthesize magnetite [1–3]. Factors that affect the characteristics of synthesized magnetite are the type of iron salt, the Fe(II)/Fe(III) ratio [4], the temperature of the reaction [5, 6], the pH [7, 8], the type of the base, and the rate of stirring [9], along with the presence of modifiers [6]. Magnetite can be synthesized by means in which only iron(II) salts are used. This approach requires the oxidation of some iron(II) cations. Sodium nitrite [8] and potassium chromate [10] can be used as oxidizing agents.

The practical significance of double oxides of iron and manganese is that the metal atoms in them can be in oxidation states +2 and +3, and manganese atoms can also be in oxidation state +4. Mixed iron and manganese oxides serve as catalysts for the oxidation of organic compounds [11–15], the decomposition of ozone [16], mechanochemical reactions [17], and oxidation while removing nitrogen oxides from the air [18]. They can be used in pulsed sources of oxygen [19], and as one of the reagents in the thermochemical production of hydrogen [20, 21]. Mixed oxides serve as electrodes for supercapacitors [22] and lithium-ion batteries [23], magnetic materials [24], and sorbents for removing arsenites and selenites from aqueous solutions [25, 26]. They can be used as solid-phase extractants in the electrochemical determination of Hg(II) [27], and as adsorbents [28–30].

Mixed iron and manganese oxides can be obtained in a number of ways. These include sintering [19, 21]; hydrothermal synthesis [16, 26]; the ultrasonic treatment of solutions [31]; precipitation from solutions

Table 1. Characteristics of the redox properties of permanganate ions

Redox reaction	n	E_o, V
$MnO_4^- + 4H^+ = MnO_2 + 2H_2O$	3	+1.695
$MnO_4^- + 8H^+ = Mn^{2+} + 4H_2O$	5	+1.51
$MnO_4^{2-} + 2H_2O = MnO_2 + 4OH^-$	2	+0.60
$MnO_4^- + 2H_2O = MnO_2 + 4OH^-$	3	+0.588
$MnO_4^- = MnO_4^{2-}$	1	+0.564
$Mn^{2+} = Mn$	2	−1.18

n is the number of electrons; E_o is the standard oxidation potential.

[25] and microemulsions [32]; electrochemically on the surfaces of electrodes [22]; and single-gel technology [24], and other methods [33].

The aim of this work was to study the physicochemical properties of condensed products resulting from the redox reaction between iron(II) cations and permanganate ions, and to determine their sorption properties with respect to highly toxic chromate anions.

EXPERIMENTAL

Reagents

In our experiments, we used a 20% ammonia solution, a solution of iron(II) sulfate (32.0 g/L) with 0.37 mol H_2SO_4/1 mol Fe(II) added to suppress hydrolysis, and a solution of potassium permanganate with a concentration of 870 mg/L.

Synthesis

Solution of iron(II) sulfate (1 mL, 11.7 mg of Fe(II)) and a predetermined volume of a solution of potassium permanganate were placed into a test tube. After stirring, 1 mL of a 20% ammonia solution was added. The volume of the solution was adjusted to 25 mL with distilled water while stirring. Condensation was conducted at room temperature or in a Lauda Alpha A12 thermostat at 30, 40, 50, 60, and 70°C. At certain time intervals, we measured the volume of sediment (V, mL), recorded the readings from an apparatus constructed on the base of an electronic analytical balance, and calculated the relative magnetic susceptibility (RMS, g/g Fe) [34].

The preparations for studying the phase composition and magnetic properties were synthesized at 20 and 100°C. The potassium permanganate/iron(II) molar ratio was varied from 0.08 to 0.32. To begin with, 100 mL of a solution prepared from 5 g iron(II) sulfate heptahydrate and 1 mL of concentrated sulfuric acid was mixed with 100 mL of a solution containing a specific weighed portion of potassium permanganate. Then 18 mL of a 20% aqueous ammonia solution were added. The period of condensation was 30 min. The precipitated condensation product was separated from the solution, washed in a centrifuge, and dried in a vacuum desiccator to a constant weight.

Magnetic Granulometry

Magnetic characteristics were measured via magnetic granulometry, which allowed us to study the chemical transformations in situ [35]. Isolated solid samples in amounts of 20 mg were loaded into the measuring cell of a vibrating magnetometer that was a flow-through quartz microreactor; specific magnetization (σ) was measured as a function of magnetic field strength H (field dependences) in an argon atmosphere. Using special software based on field dependences, the magnetic characteristics of the samples were then determined at 20°C.

Diffractometry

The phase composition of the powders of the isolated products was analyzed on a Shimadzu XRD-7000 S X-ray diffractometer. The X-ray diffraction pattern of each sample was recorded in a standard holder with a rotation of 30 rpm. The optical scheme of the goniometer (a scintillation detector with a monochromator) was θ–θ. The parameters of X-ray tube operation were accelerating voltage 40 kV, current 30 mA, and copper anode. The range of scanning was 2θ 10°–95°, and the speed of scanning was 1 deg/min with a step of 0.02°.

Scanning Electron Microscopy

Micrographs of the samples were obtained on a Sigma VP Zeiss scanning electron microscope (SEM) (accelerating voltage 10 kV; InLens detector). An Oxford 80 mm^2 energy dispersive spectrometer (accelerating voltage, 20 kV) was used to determine their elemental composition.

RESULTS AND DISCUSSION

To synthesize magnetite from an iron(II) salt, 2/3 of the iron(II) cations must be oxidized. Potassium permanganate can be used as an oxidizing agent. Depending on the initial oxidation state and the pH of the solution, manganese ions participate in redox transformations with the transfer of different numbers of electrons (Table 1) [1].

If permanganate ions act as a five-electron oxidizers in an acidic medium, the consumption of potassium permanganate during oxidation must be 1 mol per 7.5 mol of iron(II) to achieve a Fe(II)/Fe(III) ratio of 1 : 2. Chemical processes that occur under the con-

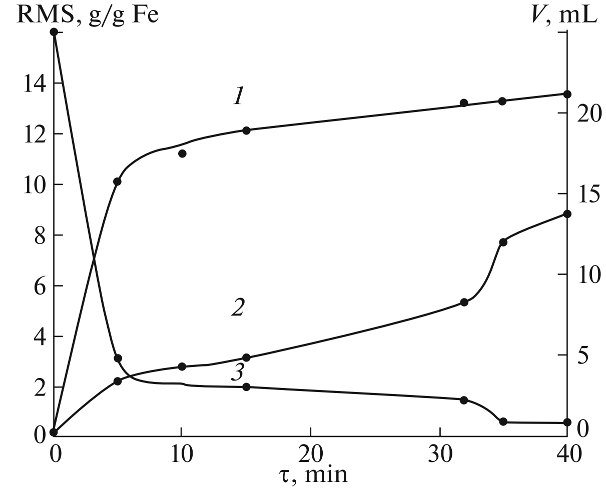

Fig. 1. Dynamics of RMS formation during condensation (*1*) on a neodymium magnet, (*2*) under natural conditions, and (*3*) dynamics of sedimentation.

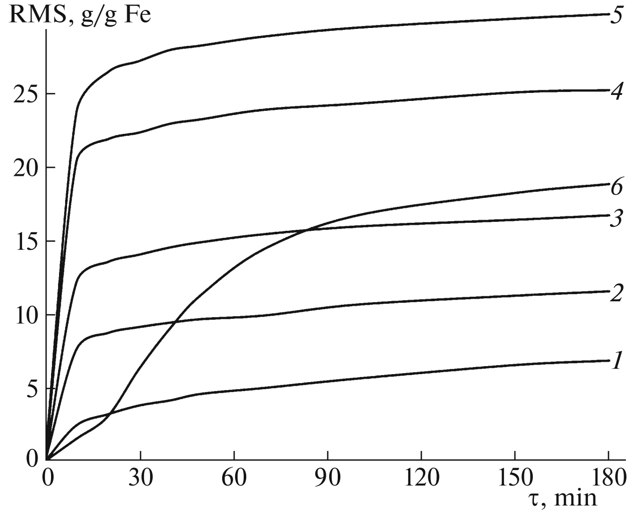

Fig. 2. Dynamics of the formation of RMS at $KMnO_4$: Fe(II) molar ratios of (*1*) 0.05, (*2*) 0.08, (*3*) 0.11, (*4*) 0.13, (*5*) 0.16, and (*6*) 0.18.

ditions of synthesis are represented by the partial oxidation of iron(II) cations proceeding in an acidic medium:

$$15FeSO_4 + 2KMnO_4 + 8H_2SO_4 = 5Fe_2(SO_4)_3$$
$$+ 5FeSO_4 + 2MnSO_4 + K_2SO_4 + 8H_2O.$$

The transfer of a single electron in an acidic medium is represented by the scheme

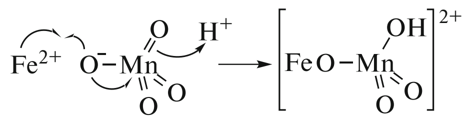

When an alkaline reagent is added to the reaction mixture, the iron hydroxide complex first precipitates:

$$Fe^{2+} + 2Fe^{3+} \xrightarrow[\text{excess}]{OH^-} Fe(OH)_2 \cdot [Fe(OH)_3]_2\downarrow.$$

Due to the dehydration of the complex, ferritization then occurs with the formation of a magnetite phase:

$$Fe(OH)_2 \cdot [Fe(OH)_3]_2 \rightarrow Fe_3O_4 + 4H_2O.$$

Under the conditions of condensation, manganese(II) hydroxide is also precipitated and included in the magnetically active compound:

$$Mn^{2+} \xrightarrow[\text{excess}]{OH^-} Mn(OH)_2\downarrow.$$

We first performed experiments with a molar ratio of permanganate ion to iron(II) equal to 0.13. In an acidic medium, the redox reaction occurred instantly. Condensation was conducted under natural conditions and on a neodymium magnet. Condensation was monitored by measuring RMS, and sedimentation was determined from the value of the precipitate volume. Figure 1 shows the results. The rate of sedimentation slowed considerably 5 min after the onset of condensation, and the RMS continued to grow over time. The measured value of the RMS depended on two components. On the one hand, a growing amount of the complex's precipitate (a concentrate) lies within the area of the measuring unit's permanent magnet. On the other hand, the formation of a magnetically active phase (a chemical process) proceeds in the solid phase. It is difficult to separate these two processes. After the stage of fast sedimentation, which is observed during the first 5–8 min, the volume of the sediment changes slowly. At this stage, the main process is the formation of the magnetically active phase (Fig. 1). When conducting condensation under natural conditions, the reaction tube was positioned on a neodymium magnet at the 31st min. This slightly lowered the volume of sediment of the condensation product (Fig. 1, curve *3*) and considerably raised the RMS (Fig. 1, curve *2*). With condensation on a neodymium magnet, sedimentation occurred within 1–1.5 min (the curve is not shown in Fig. 1, since it merges with the axes); i.e., its contribution to the measured value of the RMS was minimal. In both cases, the tubes were kept on a neodymium magnet for 48 h, and their RMSs were the same.

To reduce the effect of sedimentation, subsequent experiments were performed in such a way that the volume of the reaction mixture was not brought to 25 mL after adding a condensing reagent, and the tube was kept on a neodymium magnet for 1.5 min. In most cases, rapid sedimentation occurred during this time. The obtained dependences of the RMS on the period of condensation are of the same type (Fig. 2). The RMS grew rapidly within 10–15 min, after which the rate of the process slowed considerably. Some differences were observed in the experiment with the maximum consumption of potassium permanganate. On

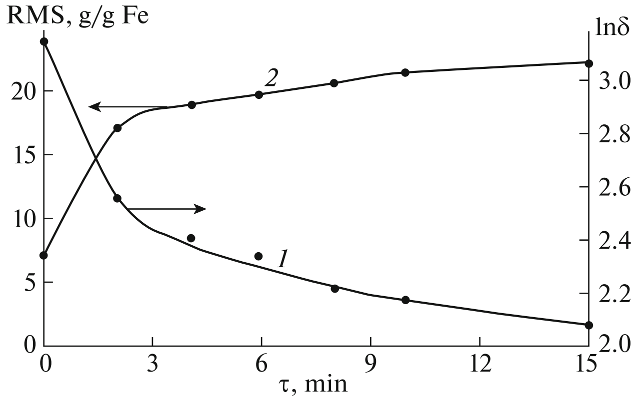

Fig. 3. Dependences of RMS and $\ln(\mathrm{RMS_{lim}} - \mathrm{RMS}_i)$ ($\ln\delta$) on the duration of condensation at 50°C. $\mathrm{RMS_{lim}}$ is the RMS limit value.

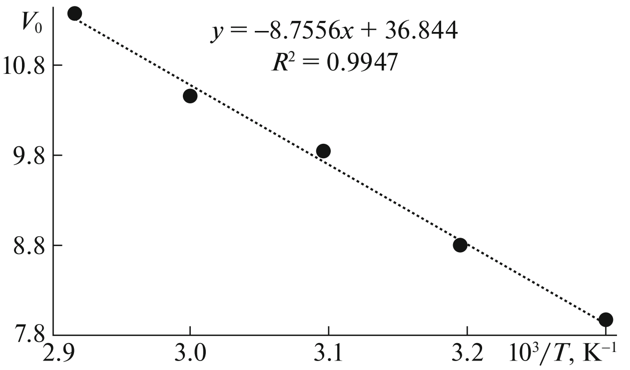

Fig. 4. Dependence of the initial rate (V_0) of RMS formation on the inverse thermodynamic temperature ($10^3/T$).

the kinetic curve, there was a rapid increase in the RMS after the period of induction, due probably to sedimentation proceeding slowly on the neodymium magnet. A gradual rise in the RMS was observed for 48 h. As a result, the maximum RMS of samples synthesized at molar ratios of potassium permanganate and iron(II) sulfate of 0.13 and 0.16 reached almost the same value of 30.3 ± 0.9 g/g Fe.

Temperature Effect

Condensation was conducted at temperatures of 30, 40, 50, 60, and 70°C after keeping each sample on a neodymium magnet for 1.5 min at room temperature. The molar ratio of potassium permanganate to iron(II) was 0.13. The RMS of the product grew at a rate that slowed over time (Fig. 3). Kinetic equations for the first- and second-order reactions were used to describe the kinetics of RMS formation. The semilogarithmic anamorphosis of the kinetic curve at 50°C indicates that the process cannot be described with satisfactory accuracy by the equation of first-order reaction kinetics, $\ln(\mathrm{RMS_{lim}} - \mathrm{RMS}_i)$. Similar results were obtained using the 1/RMS dependence.

The initial rate of condensation was then calculated. It was found to grow with temperature. The dependence of the initial rate of RMS formation on the inverse thermodynamic temperature was a first-degree polynomial (Fig. 4).

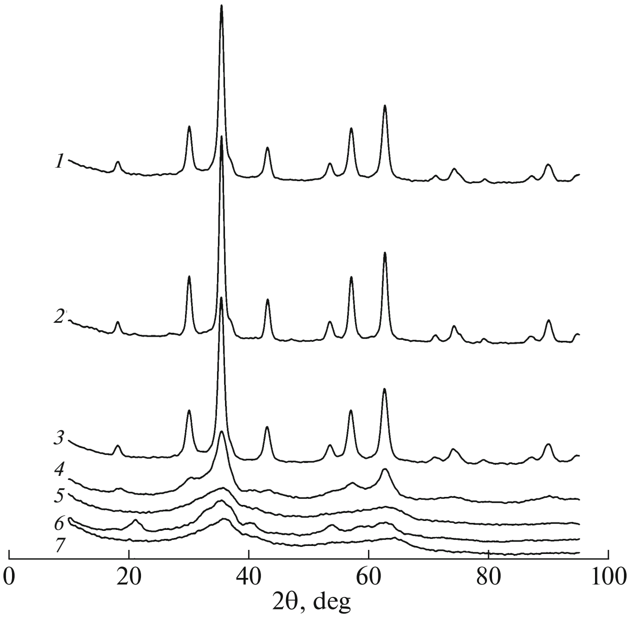

Fig. 5. Diffraction patterns of the products synthesized at $\mathrm{KMnO_4}$: Fe(II) molar ratios of (*1*, *2*) 0.08, (*3*) 0.13, (*4*) 0.18, (*5*) 0.23, (*6*) 0.27, and (*7*) 0.32. Sample *1* was condensed at 20°C; samples *2*–*7*, at 100°C.

Magnetic Characteristics

We used magnetic granulometry to determine the magnetic characteristics of products synthesized at a 0.08–0.18 molar ratio of potassium permanganate to iron(II) (Table 2). It was established that they

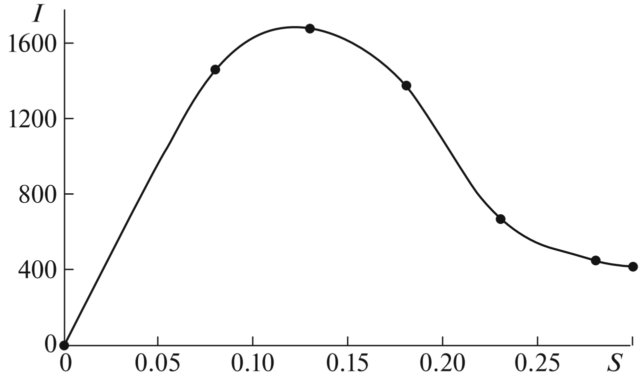

Fig. 6. Dependence of diffraction signal intensity (I) at $2\theta = 35.6°$ on the $\mathrm{KMnO_4}$: Fe(II) molar ratio (S).

Table 2. Magnetic characteristics of the reaction products

Sample	$KMnO_4$: Fe(II) molar ratio	t, °C	J_s, emu/g	J_r, emu/g	H_c, Oe	Proportion of superparamagnetic particles
1	0.08	20	130	1	0	0.985
2	0.08	100	141	0	0	1.00
3	0.13	100	81.3	1	2	0.975
4	0.18	100	38.2	1	1	0.948

belonged to superparamagnetic substances. The temperature of condensation had little effect on the magnetic characteristics of the products of condensation, which depend largely on the $KMnO_4$: Fe(II) molar ratio.

Phase Composition

X-ray diffraction patterns of the condensation products are shown in Fig. 5. There are clearly defined reflexes on the diffraction patterns of the products synthesized at a potassium permanganate-to-iron(II) molar ratio of 0.08–0.18, testifying to their crystalline structure. A comparison of the experimental diffraction patterns and those from in the PDF-2 database (Powder Diffraction File™ PDF-2 Release 2010, International Center for Diffraction Data) showed that magnetite (Fe_3O_4) was present in the product samples. The products of condensation synthesized with high consumption of potassium permanganate had an amorphous structure. The intensity of reflexes at $2\theta = 35.6°$ depended on the molar ratio and had the highest values for the samples synthesized at a potassium permanganate consumption close to the theoretical value for the formation of magnetite (Fig. 6).

Table 3. Elemental composition of the synthesized products

Sample	Element content, %		
	Fe	Mn	O
2	51.5 ± 2.1	5.5 ± 0.2	42.4 ± 2.3
3	52.5 ± 1.7	9.6 ± 0.4	37.4 ± 2.2
4	45.2 ± 8.5	11.4 ± 2.3	42.2 ± 10.8
5	38.1 ± 3.7	12.5 ± 1.4	43.4 ± 10.2
6	32.4 ± 4.6	13.8 ± 7.1	48 ± 2.1
7	34 ± 6.9	13.1 ± 2.5	52.6 ± 9.6

Morphology and Composition

The morphology and composition of the reaction products were studied via scanning electron microscopy. The composition of the selected products is presented in Table 3. A higher content of manganese in the condensation products corresponds to increased consumption of potassium permanganate in the reaction. The deviation of the total content of elements from 100% is explained small amounts of other elements being detected in the composition. Their total content did not exceed 1–1.5%.

Microphotographs of the reaction products are shown in Fig. 7. Sample 1 consists of shapeless structures formed by nanocrystals 10–20 nm in size (Fig. 7b). Sample 6 contains spherical structures 150–200 nm in size, surrounded by a shapeless amorphous mass.

Sorption

To assess the possibility of using the product synthesized at a 0.08 molar ratio of potassium permanganate to iron(II), the sorption of chromate ions was conducted under static conditions. A weighed portion of the product was mixed with a predetermined volume of potassium chromate solution at a concentration of 0.199 g/L. The resulting mixture was kept for 48 h with periodic stirring. After the experiment was complete, the precipitate was separated magnetically. The volume of supernatant was adjusted to 25 mL with distilled water, and the optical density at 375 nm was determined on an Expert 03 photometer in cuvettes with a working layer thickness of 50 mm. The optical density of the solution after sorption was 0.013; in a control experiment using the initial solution, it was 1.043. The degree of extraction of chromate ions was thus 98.7 under conditions of static sorption (coefficient of variation 0.3%; each experiment was repeated four times).

CONCLUSIONS

We studied the physicochemical properties of condensed products of interaction between iron(II) cations and permanganate ions. Depending on the molar

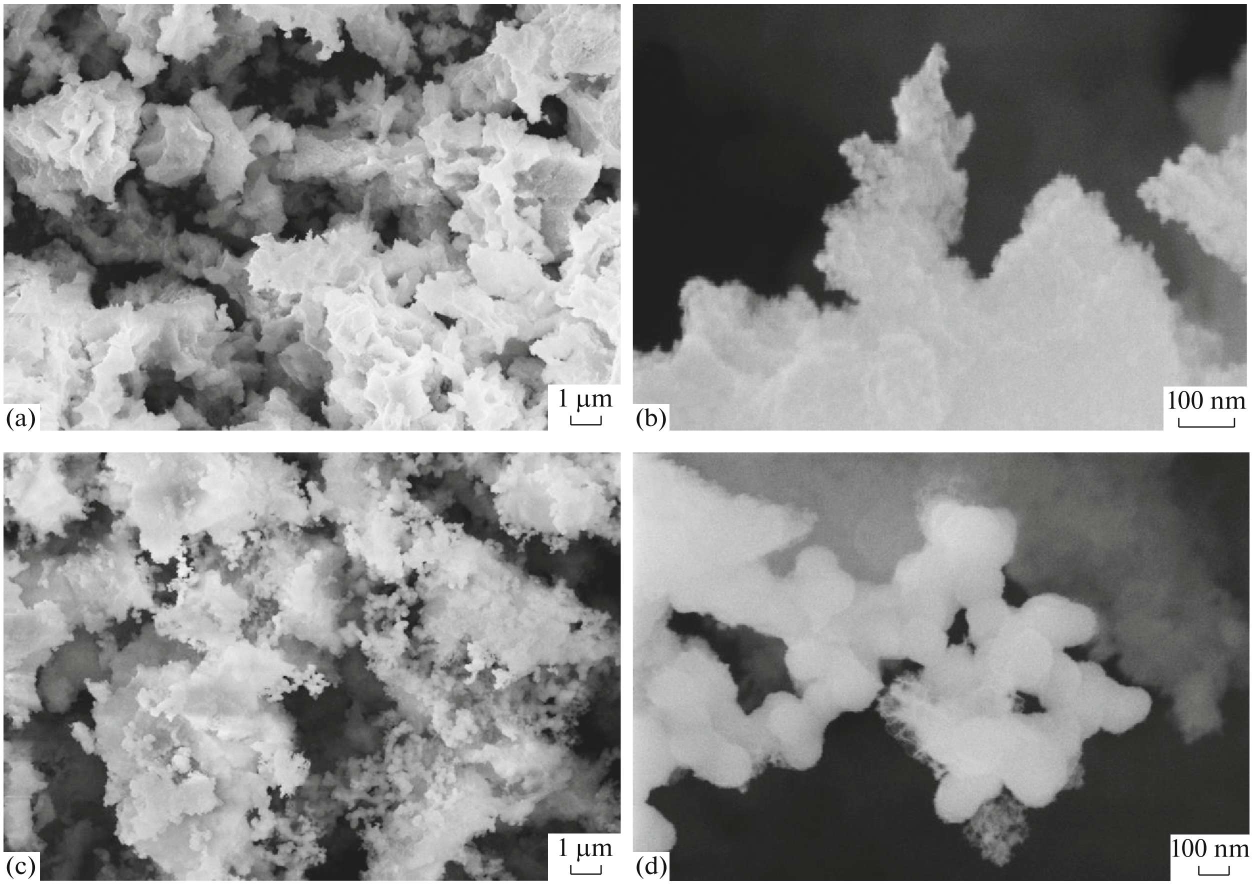

Fig. 7. Microphotographs of samples 1 (a, b) and 6 (c, d). Scale bar: (a, c) 1 μm; (b, d) 100 nm.

ratio of iron(II) cations and permanganate ions, products formed that differed in crystallinity, phase composition, and magnetic properties. Upon the partial oxidation of 2/3 of the iron(II) cations, a product with superparamagnetic properties formed during condensation. This product extracted chromate ions from aqueous solutions quite well.

ACKNOWLEDGMENTS

This work was performed on equipment at the *Arktika* shared resource center of Northern (Arctic) Federal University.

REFERENCES

1. J. A. Lopez, F. Gonzalez, F. A. Bonilla, et al., Rev. Latinoam. Metall. Mater. **30**, 60 (2010).
2. X. Sun, K. Sun, and Y. Liang, Micro Nano Lett. **10**, 99 (2015). https://doi.org/10.1049/mnl.2014.0344
3. P. L. Hariani, M. Faizal, R. Marsi, et al., Int. J. Environ. Sci. Devel. **4**, 336 (2013). https://doi.org/10.7763/IJESD.2013.V4.366
4. T. Hyeon, Chem. Commun., No. 8, 927 (2003). https://doi.org/10.1039/B207789B
5. A. Ditsch, P. E. Laibinis, D. I. C. Wang, et al., Langmuir **21**, 6006 (2005). https://doi.org/10.1021/la047057+
6. H. Hosseini-Monfared, F. Parchegani, and S. Alavi, J. Colloid Interface Sci. **437**, 1 (2015). https://doi.org/10.1016/j.jcis.2014.08.056
7. R. Massart, IEEE Trans. Magn. **17**, 1247 (1981). https://doi.org/10.1109/TMAG.1981.1061188
8. I. Nedkov, T. Merodiiska, S. Kolev, et al., Monatsh. Chem. **133**, 823 (2002). https://doi.org/10.1007/s007060200054
9. K. A. Subbotin, A. I. Mikhailichenko, and N. V. Nefedova, Russ. J. Appl. Chem. **73**, 1671 (2000).
10. Yu. G. Khabarov, N. Yu. Kuzyakov, V. A. Veshnyakov, A. V. Malkov, N. V. Shkaeva, and G. V. Pankina, Russ. J. Inorg. Chem. **62**, 231 (2017).
11. F. G. Duran, B. P. Barbero, L. E. Cadus, et al., Appl. Catal. B: Environ. **92**, 194 (2009). https://doi.org/10.1016/j.apcatb.2009.07.010
12. S. Nicolae, F. Neatu, and M. Florea, C. R. Chim. **21**, 354 (2018). https://doi.org/10.1016/j.crci.2017.06.005
13. P. Mungse, G. Saravanan, S. Rayalu, et al., Energy Technol. **3**, 856 (2015). https://doi.org/10.1002/ente.201500035

14. J. Zhu, S. A. Baig, T. Sheng, et al., J. Hazard. Mater. **286**, 220 (2015). https://doi.org/10.1016/j.jhazmat.2015.01.004
15. J. Chen, X. Chen, W. Xu, et al., Chem. Eng. J. **330**, 281 (2017). https://doi.org/10.1016/j.cej.2017.07.147
16. Z. Lian, J. Ma, and H. He, Catal. Commun. **59**, 156 (2015). https://doi.org/10.1016/j.catcom.2014.10.005
17. M. M. Barroso Quiroga, B. P. Barbero, and L. E. Cadus, Appl. Catal., A **474**, 26 (2014). https://doi.org/10.1016/j.apcata.2013.09.001
18. G. Qi and R. T. Yang, Appl. Catal., B **44**, 217 (2003). https://doi.org/10.1016/S0926-3373(03)00100-0
19. A. Shafiefarhood, A. Stewart, and F. Li, Fuel **139**, 1 (2015). https://doi.org/10.1016/j.fuel.2014.08.014
20. L. I. Kuklo, S. I. Belyaninova, S. S. Ermakov, et al., Appl. Phys. A **82**, 599 (2006). https://doi.org/10.1007/s00339-005-3401-3
21. P. B. Kreider, H. H. Funke, K. Cuche, et al., Int. J. Hydrogen Energy **36**, 7028 (2011). https://doi.org/10.1016/j.ijhydene.2011.03.003
22. M. T. Lee, J. K. Chang, Y. T. Hsieh, et al., J. Power Sources **185**, 1550 (2008). https://doi.org/10.1016/j.jpowsour.2008.09.007
23. Z. Zhang, Y. Ji, J. Li, et al., ACS Appl. Mater. Interfaces **7**, 6300 (2015). https://doi.org/10.1021/acsami.5b00617
24. J. W. Long, M. S. Logan, E. E. Carpenter, et al., J. Non-Cryst. Solids **350**, 182 (2004). https://doi.org/10.1016/j.jnoncrysol.2004.06.036
25. G. Zhang, F. Liu, H. Liu, et al., Environ. Sci. Technol. **48**, 10316 (2014). https://doi.org/10.1021/es501527c
26. M. Szlachta, V. Gerda, and N. Chubar, J. Colloid Interface Sci. **365**, 213 (2012). https://doi.org/10.1016/j.jcis.2011.09.023
27. M. Fayazi, M. A. Taher, D. Afzali, et al., Sens. Actuators, B **228**, 1 (2016). https://doi.org/10.1016/j.snb.2015.12.107
28. X. Luo, C. Wang, S. Luo, et al., Chem. Eng. J. **187**, 45 (2012). https://doi.org/10.1016/j.cej.2012.01.073
29. A. Buccolieri, A. Serra, G. Maruccio, et al., J. Anal. Methods Chem. **2017**, 9476065 (2017). https://doi.org/10.1155/2017/9476065
30. C. L. Warner, W. Chouyyok, K. E. Mackie, et al., Langmuir **28**, 3931 (2012). https://doi.org/10.1021/la2042235
31. J. Lai, K. Shafi, A. Ulman, et al., J. Phys. Chem. B **108**, 14876 (2004). https://doi.org/10.1021/jp049913w
32. T. Herranz, S. Rojas, M. Ojeda, et al., Chem. Mater. **18**, 2364 (2006). https://doi.org/10.1021/cm052568i
33. L. I. Kuklo, S. I. Belyaninova, S. S. Ermakov, et al., Nanotechnol. Russ. **11**, 137 (2016). https://doi.org/10.1134/S1995078016020105
34. Yu. G. Khabarov, I. M. Babkin, and V. A. Veshnyakov, Russ. J. Appl. Chem. **85**, 883 (2012). https://doi.org/10.1134/S1070427212060080
35. P. A. Chernavskii, G. V. Pankina, and V. V. Lunin, Russ. Chem. Rev. **80**, 579 (2011). https://doi.org/10.1070/RC2011v080n06ABEH004187

Translated by G. Levit